POWER AND ENERGY FUTURE

Open Access

Research Article

Research on Time-of-Use Pricing Optimization and Load Adjustment in Distributed Energy Systems

XiuYu Zhang, Jin Sun, Xinkai Chen, and LinCheng Han

***Abstract*—To address the challenges of integrating high proportions of renewable energy into the grid amid the energy transition, this paper proposes a time-of-use pricing-based electricity optimization model for distributed wind-solar hybrid systems. The model aims to guide load demand through price signals, achieving synergistic optimization of efficient energy consumption and economical system operation. To address the limitations of traditional single-objective optimization, this study constructs a multi-objective optimization framework centered on maximizing wind power consumption and minimizing operational costs. A hybrid optimization strategy integrating the hierarchical evolution algorithm (HEA) and tabu search (TS) is designed to enhance global search capability and convergence efficiency. The model comprehensively considers key conditions such as power balance constraints, dynamic characteristics of energy storage systems, and equipment operational limitations, establishing a systematic power output and multi-objective optimization function. Simulation results demonstrate that the proposed method effectively smooths load curves, enhances grid stability, and significantly improves renewable energy utilization rates. This research offers an innovative solution for balancing renewable energy integration with economic efficiency within electricity market environments, validating the practical application potential of time-of-use pricing strategies in advancing energy internet development.**

***Index Terms*—Distributed power, time-of-use tariffs, wind energy consumption, hierarchical evolutionary algorithms, tabu search.**

ABBREVIATION

PV	photovoltaic
HEA	hierarchical evolutionary algorithm
TS	tabu search
DR	demand response
TOU	time-of-use
FOC	first-order condition
GA	genetic algorithm
IR	improvement rate
SD	search diversity
CEO	chaotic evolutionary optimization
BHD	bidirectional Hausdorff distance
HV	hypervolume
GD	generation distance

Manuscript received 26 September, 2025; revised 10 October, 2025; accepted 28 October, 2025. *(Corresponding authors: Xinkai Chen, e-mail: chen@shibaura-it.ac.jp and LinCheng Han, e-mail: 1202100043@neepu.edu.cn)*

X. Zhang, J. Sun and L. Han are with the School of Automation Engineering Northeast Electric Power University.

X. Chen is with the Department of Electronic and Information Systems, Shibaura Institute of Technology.

Color versions of one or more of the figures in this paper are available online at https://doi.org/10.26599/PEF.2025.9650002.

Digital Object Identifier 10.26599/PEF.2025.9650002

I. INTRODUCTORY

With the promotion of the energy revolution and digital transformation, as well as the deepening of the power system reform, the power system is being rapidly upgraded, and is gradually developing into an "energy Internet" integrated with the Internet [1]. In this process, distributed power (DG) as the main form of renewable energy access, due to its modularity, flexibility, and low-carbon characteristics, has become the core carrier of the global energy transition. Taking Germany as an example, its distributed photovoltaic penetration rate has exceeded 30%, and the renewable energy consumption rate has been increased by 15% through the time-sharing tariff mechanism, which verifies the key role of the market mechanism on the development of DG [2]. In the context of the expansion of China's electricity market, the planning and operation of DG has gradually shifted from distribution companies to be carried out independently by DG operators. This shift brings new challenges: On the one hand, the stochastic and fluctuating nature of DG leads to frequent distribution network voltage overruns (e.g., consumption conflicts caused by the overlap of peak PV output and grid valley tariffs in Shandong [3]); on the other hand, the distribution company, as an active distribution network operator, needs to balance the interests of multiple parties through dynamic optimization strategies. The study shows that the use of time-sharing tariff optimization model based on net load curve can improve the PV acceptance capacity of distribution network by 4.75% [4], highlighting the technical value of tariff mechanism design.

As a demand-side management tool in the electricity market, time-sharing tariff centers on reconfiguring the elasticity of user electricity consumption through tariff signals. References

[5], [6] discuss the technical changes brought by the smart grid to demand side management from the perspective of demand response, pointing out that the smart grid realizes two-way interaction between the power system and the users through advanced communication, automation, and information technology, so as to more accurately guide the users to respond to the tariff signals and optimize their electricity consumption behaviors, and puts forward the construction steps and suggestions for demand side management. The 5-min real-time tariff mechanism implemented in California, USA, has successfully shifted peak loads by 22% through fast-response tariff adjustments [7], while in Germany, industrial customer load responsiveness was increased to 40% through interruptible tariff agreements [2]. These cases fully demonstrate the remarkable effect of real-time tariff mechanism in demand-side management, which can effectively alleviate the peak-to-valley difference of the power system and improve the system operation efficiency. Based on the deterministic or uncertainty model of load demand response, [8] has established an optimization objective function and thoroughly studied the impact of different tariff strategies on distributed energy consumption. It provides theoretical support for the development of scientific and reasonable tariff policy, which helps to better integrate distributed energy and improve energy utilization efficiency. References [9], [10], [11] further analyzes the impact of time-sharing tariffs and marginal tariff differential costs on user behavior, and puts forward the principles and constraints of tariff development that ensure adequate grid integration and consumption of distributed energy while affecting the stable operation of the electricity market. However, there are many shortcomings in the existing time-sharing tariff research. First, pricing methodology limitations. Most studies focus on the time-sharing tariff characteristics of specific electricity markets, but the complexity and diversity of distributed energy systems are not sufficiently considered. Peak tariff hours do not coincide with the peak hours of renewable energy generation (e.g., the overlap of PV output and valley tariff in Shandong [3]), but instead inhibit the user demand for electricity. Second, the optimization algorithm is inefficient. Existing algorithms (e.g., NSGA-II algorithm [12]) suffer from slow computation speed and parameter sensitivity when dealing with large-scale systems, while hybrid algorithms (linear programming + particle swarm optimization [13]) reduce the complexity but do not solve the problem of dynamic adaptation of distributed energy output. Finally, the system modeling is one-sided. The equivalent load model proposed in [14] improves PV consumption, but does not consider the energy storage charging and discharging frequency constraints.

For this reason, this paper proposes a distributed wind and solar combined system consumption model based on time-of-use tariffs, aiming to guide the load demand by adjusting the tariffs to promote the maximization of wind and solar energy consumption and minimize the cost. This study deeply analyzes the characteristics of distributed energy system and time-sharing tariff mechanism, takes into full consideration of the output characteristics of different types of energy, cost differences, and user demand response characteristics, constructs a more scientific and reasonable pricing model, optimizes the pricing process, and improves the reasonableness and scientificity of time-sharing tariff. In addition, combined with the characteristics of renewable energy generation and load characteristics, a matching time-sharing tariff scheme is designed to ensure the provision of reasonable tariff incentives during the peak hours of renewable energy generation and to promote its effective utilization. This paper expects to provide a more targeted and effective solution for time-of-day tariff optimization and load regulation of distributed energy systems, and to provide an innovative method for the electricity market that can both promote renewable energy consumption and ensure economic benefits.

II. Time-of-Use tariff pricing methodology process

The aim of this thesis is to explore time-of-day tariff optimisation and load regulation strategies in distributed energy systems, aiming to achieve efficient energy distribution and cost control. The paper introduces the process of time-of-day tariff pricing methodology, including key steps such as data collection, demand response analysis, and time slot division, which provides the basis for the construction of the subsequent optimisation model. As shown in Fig. 1, the overall framework of the paper demonstrates the research process from data collection to simulation and analysis.

In the data collection stage, this study combines load demand and meteorological data, which lays the foundation for subsequent analyses. Based on these data, the *K*-means clustering algorithm is used to classify the load data and divide the time periods [14] into peak, flat, and low time periods, which provides a scientific basis for the development of time-sharing tariffs.

In order to further optimise the time-of-use tariff, this paper constructs a multi-objective optimisation model aiming to maximise the wind power output and minimise the operating costs. To solve this optimisation problem, a hybrid optimisation strategy combining a HEA and a TS algorithm is proposed. This method not only meets the grid operation requirements, but also improves the system performance while taking into account the economic and environmental benefits. One of the core contents of the paper is to explore the conver-

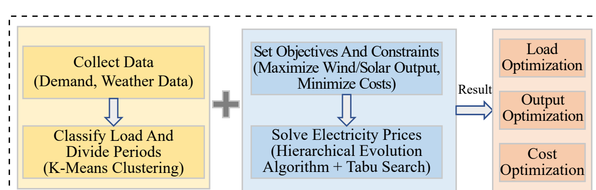

Fig. 1. Overall flow of the thesis.

gence mechanism of HEA and TS. HEA maintains the population diversity and accelerates the convergence speed through the hierarchical mechanism; meanwhile, the tabu search enhances the local search capability and avoids falling into the local optimal solution, thus improving the global search accuracy.

In terms of distributed energy system modelling, this paper constructs a power output model in detail and designs a multi-objective optimization function, specifying key conditions such as power balance, energy storage system, and equipment operation constraints. Through simulation analysis, the effectiveness of the proposed method is verified, and the changes in load demand curves, equipment output, and cost allocation after optimisation are demonstrated, which further proves the role of time-of-day tariff optimisation strategy in balancing the load demand and enhancing the stability of the power grid.

In summary, this paper systematically investigates the time-sharing tariff optimisation and load regulation methods through theoretical analyses and simulation experiments, which provides new perspectives and innovative solutions for achieving sustainable energy management and efficient operation of power grids.

III. Load Classification and Time Period Classification

A. Electricity Load and Demand Response Mechanisms

The dynamic changes in electric load are significantly influenced by seasons, climate, and consumer behavior, resulting in distinct spatiotemporal heterogeneity. To analyze the load fluctuation characteristics, this study uses a clustering algorithm to classify historical load data into three seasonal categories: spring-autumn, summer, and winter. This approach helps reveal seasonal load distribution patterns and their impacts on grid regulation.

DR [15] serves as a critical load optimization tool, with its core economic principle rooted in reflecting the true marginal cost of electricity across different time periods through price signals. It leverages users' price elasticity of demand to guide electricity consumption behavior. The marginal cost of electricity supply in power systems fluctuates significantly over time: During peak loads, costly peak-shaving units must be deployed, resulting in high marginal costs; during off-peak periods, marginal costs are primarily determined by low-cost base-load units. TOU pricing specifically aims to pass this temporal cost differentiation to consumers. Its microeconomic essence lies in consumers' rational choice to maximize their own utility under budget constraints [16].

The theoretical foundation for users' response behavior to electricity prices stems from consumer choice theory in microeconomics. Assuming that users derive utility from electricity consumption, their decision-making over T time periods can be described by solving the following utility maximization problem:

$$\begin{aligned} \max_{d_1,\cdots,d_T} \quad & U(d_1,d_2,\cdots,d_T) \\ \text{s.t.} \quad & \sum_{t=1}^{T} M_t d_t \le I \end{aligned} \tag{1}$$

where M_t is the electricity price in period t, d_t is the electricity consumption in period t, and I is the consumer's total electricity budget.

The theoretically exact demand function is derived by constructing the Lagrangian function:

$$\mathcal{L} = U(\boldsymbol{d}) - \lambda\left(\sum_{t=1}^{T} M^t d^t - I\right) \tag{2}$$

and solving the FOC, yielding:

$$\frac{\partial U}{\partial d^t} = \lambda M^t, \quad \forall t = 1,2,\cdots,T \tag{3}$$

This system of equations implicitly defines the optimal electricity consumption d^{*t} as a function of the electricity price vector $\boldsymbol{M}$, that is, $d^{*t} = f^t(M^1, M^2, \cdots, M^T)$. However, two major obstacles hinder the engineering application of this theoretical model: (1) Unobservable utility function: The user's true utility function $U(\cdot)$ is private information and cannot be directly observed or specified. (2) Curse of dimensionality: The demand function f^t depends on electricity prices across all time periods. Consequently, demand changes in any given period are influenced by the entire price system, resulting in excessive model complexity.

To overcome these challenges, a reasonable and practical simplification of the theoretical model is required. This paper employs a local linear approximation approach that focuses on load transfer behavior between two specific time periods, i and j. Under the assumption that electricity prices and consumption in all other periods remain constant, the user's optimal consumption decisions (d^i, d^j) in these two periods depend solely on (M^i, M^j). By applying total differentiation to the first-order condition and decomposing it via the Slutsky equation, the approximate relationship between the load transfer amount from period i to j, denoted $\Delta d_{i,j}$, and the electricity price difference between the two periods, $\Delta M_{i,j}$, is derived as:

$$\Delta d_{i,j} \approx \underbrace{\left(\left. \frac{\partial d^i}{\partial M^j} \right|_{\bar{U}} \right)}_{\epsilon_{i,j}} \cdot \Delta M_{i,j} \tag{4}$$

where $\epsilon_{i,j}$ represents the cross-price elasticity coefficient from period i to j, defined as the rate of change in electricity consumption in period i in response to a one-unit change in the electricity price of period j. To scale the response amount relative to the actual load, it is standardized using the average load $\bar{D}_i$, leading to the following linear response model commonly adopted in engineering applications:

$$\Delta d_{i,j} = \epsilon_{i,j} \cdot \bar{D}_i \cdot \Delta M_{i,j} \tag{5}$$

Although linear models are simple, their direct application to real-world systems still requires consideration of three types of physical or behavioral economic constraints: First, load transfer between periods i and j occurs only if the price difference exceeds the perception threshold $M^{\alpha}_{i,j}$, i.e., $|\Delta M_{i,j}| > M^{\alpha}_{i,j}$. Second, the amount of shifted load is capped by the physical capacity $\lambda^{\alpha}_{i,\max}\bar{D}_i$. Third, to simplify dispatch, the day is aggregated into three tariff bands, peak, flat, and valley, denoted by $\alpha \in \{\mathrm{pu, pf, fu}\}$; the model therefore considers inter-band shifts rather than exchanges between arbitrary instants.

After introducing these constraints, the linear model is revised into a more practical piecewise linear form. By defining the load transfer rate $\lambda_{i,a} = \Delta d_{i,j}/\bar{D}_i$, we obtain the core response model of this paper, which has clear economic implications:

$$\text{Let } \Delta M^{\text{sat}}_a = \frac{\lambda_{i\max,a}}{k_i} + M_{i4,a} \tag{6}$$

$$\lambda_{i,a} = \begin{cases} 0 & 0 \le \Delta M_a \le M_{i4,a} \\ k_{i,a}(\Delta M_a - M_{i4,a}) & M_{i4,a} \le \Delta M_a \le \Delta M^{\text{sat}}_a \\ \lambda_{i\max,a} & \Delta M_a \ge \Delta M^{\text{sat}}_a \end{cases} \tag{7}$$

where $\lambda_{i,a}$ is the load transfer rate at node i in response to the peak, valley, and level tariff difference, i.e., the proportion of load demand shifted from the high tariff period to the low tariff period. $a = pv$ represents the shift from the peak period to the valley period, $a = pf$ represents the shift from the peak period to the equal time period, and $a = fv$ represents the shift from the equal time period to the valley period. ΔM_a represents the tariff difference between the peak and the valley, the valley and the peak, and the level tariffs. $M_{i4,a}$ represents the threshold of the minimum tariff difference which prompts the transfer of loads from the high to the low tariff period. $k_{i,a}$ represents the maximum load transfer rate from high to low tariff period, and represents the maximum load transfer rate from high to low tariff period. $\Delta M_a - M_{i4,a}$ denotes the rate of change of load transfer rate from high tariff period to low tariff period. $\lambda_{i\max,a}$ denotes the maximum load transfer rate from high tariff period to low tariff period.

After determining the load transfer rates $\lambda_{i,a}$ between all time periods, the new load curve after implementing time-of-use pricing can be obtained by superimposing the net transfer amounts in each period according to the law of energy conservation. Taking the peak period (T_p) as an example, its load reduction equals the sum of the amounts transferred to the valley period ($\lambda_{i,pv}D_{p,av}$) and the normal period ($\lambda_{i,pf}D_{p,av}$). Therefore, the final load adjustment model is:

$$d^t_i = d^t_{i0} + \begin{cases} -\lambda_{i,pv}D_{p,av} - \lambda_{i,pf}D_{p,av} & t \in T_p \\ +\lambda_{i,pf}D_{p,av} - \lambda_{i,fv}D_{f,av} & t \in T_f \\ +\lambda_{i,pv}D_{p,av} + \lambda_{i,fv}D_{f,av} & t \in T_v \end{cases} \tag{8}$$

where d^t_i and d^t_{i0} are the load demand of load node i at t under time-of-day tariff and conventional tariff, respectively; T_p, T_v, and T_f are the peak, valley, and flat periods of load under time-of-day tariff, respectively; and $D_{p,av}$ and $D_{f,av}$ are the average values of the load demand of load node i at peak and flat periods under conventional tariff, respectively.

By dividing the load data into different seasons and time periods and combining the demand response characteristics, this study aims to optimise the load regulation and grid management strategies to promote the rational allocation of power resources and the efficient operation of the grid.

B. Seasonal Cluster Analysis of Load Data

In power load analysis, the selection of an appropriate clustering technique is crucial for revealing the intrinsic characteristics of load data. This technique not only helps in accurate time period classification, but also promotes the formulation of load optimisation strategies. In view of the obvious seasonal changes and daily fluctuations of electricity load, this paper adopts the *K*-means clustering algorithm to classify the load data in order to analyse the load characteristics of different seasons in depth and to provide data support for the optimal allocation of electricity resources.

The fundamental innovation of our clustering methodology lies in its input feature set. Traditional methods rely solely on historical load data $L(t)$, which segments time periods from a unidirectional (demand-side) perspective and disregards supply-side characteristics. This constitutes the theoretical root cause of supply–demand mismatches.

To overcome this limitation, our model integrates both load demand and concurrent renewable energy generation characteristics into a multidimensional feature vector for clustering. Specifically, the input vector for the *K*-means algorithm is defined as:

$$\boldsymbol{x} = [L(t), G_w(t), G_{pv}(t)] \tag{9}$$

where $G_w(t)$ and $G_{pv}(t)$ are the typical daily output curves from distributed wind and photovoltaic power, respectively.

This integrated approach ensures that each segmented time period (peak, flat, and valley) mathematically embodies the combined characteristics of "high load" and "high renewable availability". For instance, an identified "peak" period is highly likely to correspond to either a "sunny afternoon with high air conditioning demand" or a "windy night with concentrated industrial electricity consumption".

This inherent coupling of supply-side and demand-side characteristics at the fundamental level of period segmentation lays a robust foundation for resolving the temporal mismatch issue. It enables the subsequent time-of-use pricing strategy to effectively guide load demand towards periods of high renewable generation, achieving a synergistic optimization of energy consumption efficiency and economical system operation.

As shown in Fig. 2, through cluster analysis, we grouped the load data into three main categories: spring and autumn loads, summer loads, and winter loads, each of which has its own unique characteristics:

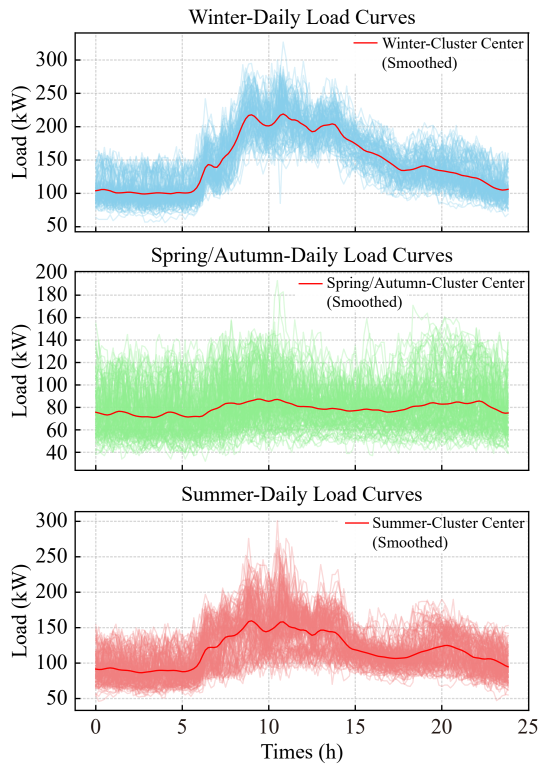

Fig. 2. Seasonal clustering.

Spring and autumn load: During these two seasons, the mild climate and relatively low residential and commercial heating and cooling demand result in a lower and less volatile overall electricity load, which is mainly influenced by daily activities.

Summer loads: Hot summer weather significantly increases the frequency of use of air conditioning and other refrigeration equipment, resulting in a significant increase in peak daytime loads, especially in the late afternoon hours.

Winter loads: Cold weather causes a surge in demand for heating equipment, especially in the evenings and early mornings, when electricity consumption often peaks.

Through this integrated clustering analysis, this paper accurately identifies the combined supply-demand characteristics of different seasons, providing a scientific basis for time slot division and tariff optimization that simultaneously considers grid stability and renewable energy utilization. In addition, the clustering results also provide strong data support for demand response and the formulation of power dispatch strategies that can effectively promote the integration of renewable resources into the distribution network.

The output of this clustering process, the division of time periods that reflect both consumption patterns and generation availability, serves as the foundational input for the subsequent development of our time-of-use pricing optimization model, which is detailed in the following sections.

C. *Method of Dividing the Time Period*

After an exhaustive discussion of seasonal load characteristics integrated with renewable generation patterns, the combined data was meticulously categorised using the *K*-means clustering algorithm. The algorithm effectively classifies the data into three distinct categories, each reflecting the co-evolving characteristics of electricity use and renewable generation availability in a particular season. This integrated clustering approach represents a fundamental departure from traditional unidimensional load-based segmentation, ensuring that the resulting time period division inherently captures the synergy between consumption patterns and generation profiles.

Through clustering analysis, it is not only able to identify the load patterns specific to each season, but also able to predict the changes in electricity demand during different time periods. These results provide a scientific basis for the development of time-sharing tariff strategies, which helps to optimise the allocation of power resources and ensure the stable operation of the power grid, while also providing users with a more reasonable cost of electricity consumption. When dividing the time periods [17], the electricity load data of different seasons are clustered to determine the peak and valley time periods. Electricity load data are simple one-dimensional data, the number of time periods and clusters is small, and the traditional *K*-means clustering algorithm can be used to meet the requirements. *K*-means clustering algorithm's objective function is the sum of the mean squared deviations of the data and the cluster centres to which it belongs. The process of determining time slots based on *K*-means clustering algorithm is shown in Fig. 3.

Based on the seasonal characteristics of the load data, it is reflected that different seasons can have a significant impact on electricity demand. Low and stable loads in spring and autumn indicate moderate temperatures and a more consistent pattern of electricity use by residents and businesses. The significant increase in load data in winter is mainly due to the rise in heating demand, especially during the night and early morning hours. Summer likewise shows higher loads, especially in the late afternoon and early evening, which is closely related to the increased frequency of air conditioning use.

As shown in Fig. 4, typical daily load profiles for the spring and autumn, winter, and summer categories are demonstrated. It is evident from the figure that each season has its own

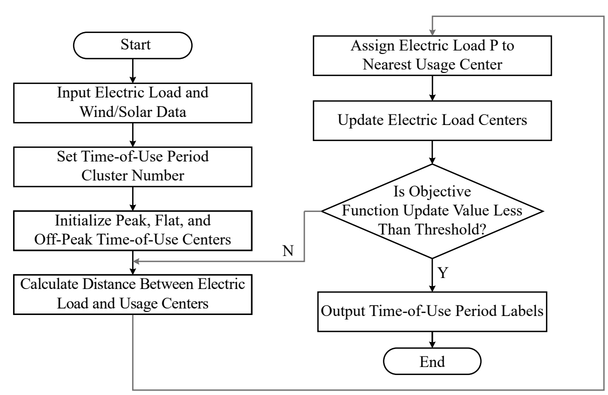

Fig. 3. Time-sharing session segmentation process.

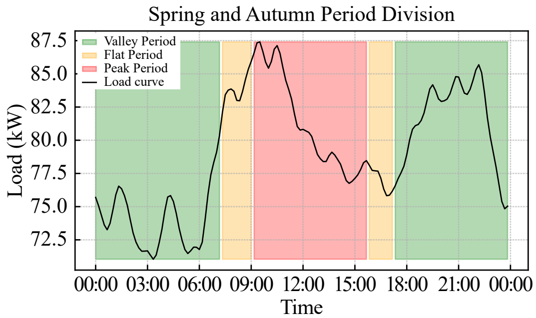

(a) Spring and Autumn

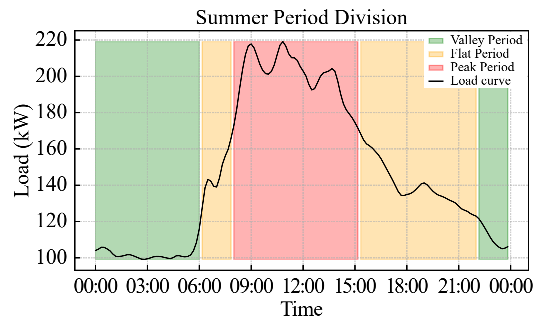

(b) Summer

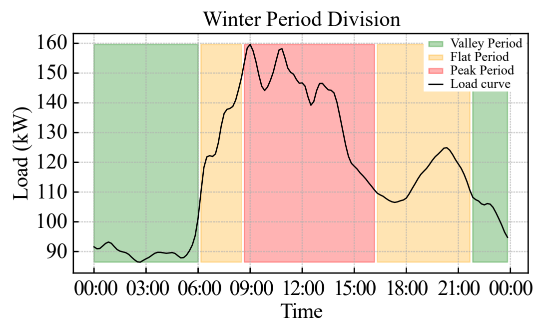

(c) Winter

Fig. 4. Evaluation metrics comparison results.

unique load patterns which are essential for the development of time-of-day tariff strategies. For example, in winter, we can observe load peaks at night and early morning, which may be related to the use of electric heating devices by residents. Whereas in summer, load peaks in the late afternoon and early evening may be associated with air-conditioning use. The time period classification of loads is mainly influenced by daily activity patterns, seasonal climatic characteristics, and energy usage habits. As shown in Fig. 4, it demonstrates the typical daily load curves of campus loads in spring and fall, winter, and summer. The time period division of the campus load from the graph is closely related to the daily rhythm of activities on campus. The concentrated periods of teaching and learning activities usually correspond to load peaks. In addition, seasonal climate change significantly affects the load characteristics, with cooling demand in summer and heating demand in winter leading to load peaks in the respective seasons. By weighting the wind and solar power outputs, it is possible to effectively guide the users to use electricity during the time when the new energy generation is high, to improve the efficiency of energy use, and to optimize the energy management.

IV. Time-of-Day Tariff Optimisation Algorithm

A. Hierarchical Evolution Combined with Taboo Search Algorithm Proposal

A new optimisation algorithm, HEA, is proposed on the basis of the traditional genetic algorithm. The algorithm divides the population into a master population and an elite population by simulating the stratification mechanism in biological evolution, where the former is responsible for searching a larger range of solution space and the latter focuses on optimising the quality of the solutions, thus accelerating the convergence process of the algorithm while maintaining the diversity of the population. In order to further enhance the local search capability of the algorithm, this paper also incorporates the TS algorithm into HEA, forming the HEA-TS algorithm. Tabu search, as a sub-heuristic stochastic search method, can effectively avoid falling into local optimal solutions, thus enhancing the global search capability of the algorithm.

B. Algorithm Principles and Steps

(1) Principle of hierarchical evolution: The traditional GA [18] relies on a single global search strategy, which is susceptible to the limitation of local search capability, affecting its efficiency and convergence. To overcome this problem, HEA introduces a hierarchical structure on the basis of genetic algorithm, divides the population into main and elite populations, and employs a targeted optimisation strategy by dividing the different levels of the solution space, which enhances the global search capability and avoids local optimal solutions.

The core idea of the hierarchical evolutionary algorithm is to explore the solution space through the collaborative work of the main and elite populations. The main population performs global search, using looser operations (e.g., wide range of variants and low selection pressure) in order to extensively explore the solution space, while the elite population focuses on local optimisation, using precise search strategies to deeply improve the current solution. Search operations at each level are performed in different regions of the solution space to progressively approximate the optimal solution.

As shown in Fig. 5, the basic framework of the hierarchical evolutionary algorithm is demonstrated, which visually presents how the main and elite populations collaborate and the optimisation strategies at different levels.

(2) Tabu search algorithm: TS [19] is an efficient heuristic algorithm commonly used in combinatorial optimisation problems. Its core idea is to find better solutions through local search and introduce a tabu mechanism to avoid falling into local optimal solutions, so as to improve the diversity and efficiency of the search. Tabu search continuously explores in the solution space by updating the search path and avoids repeated

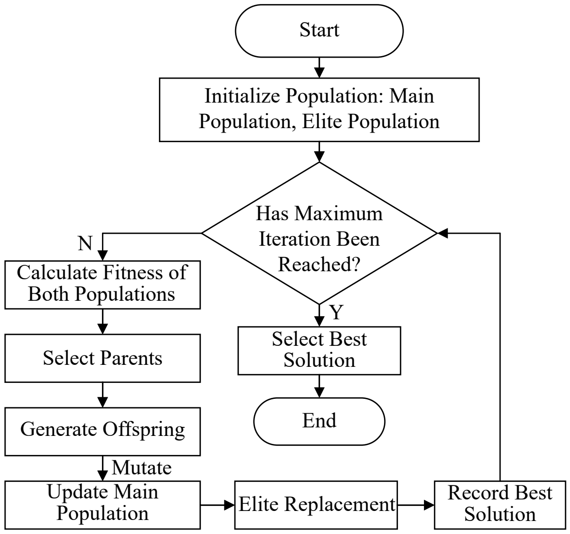

Fig. 5. Flow of hierarchical evolutionary algorithm.

visits to the explored solutions.

The key feature of tabu search is the tabu mechanism, which records the most recently accessed solutions or operations and prohibits them from being accessed again for a short period of time. With the tabu table, the algorithm stores the visited solutions or operations and excludes them for a certain period of time, avoiding ineffective repeated searches and thus avoiding locally optimal solutions.

In each search, the forbidden search defines the neighbourhood structure according to the needs of the problem and generates multiple candidate solutions. The definition of the neighbourhood is flexibly adjusted according to the specific problem to ensure the diversity of the solution space. During the search process, the current solution is updated by selecting the optimal solution from the neighbourhood of the current solution. Even if a solution is marked as tabu, it can still be accepted if it is better than the current optimal solution. This mechanism allows tabu search to not only avoid local optimal solutions, but also effectively explore global optimal solutions.

As shown in Fig. 6, the basic flow of the forbidden search algorithm is demonstrated to help intuitively understand its operation mechanism:

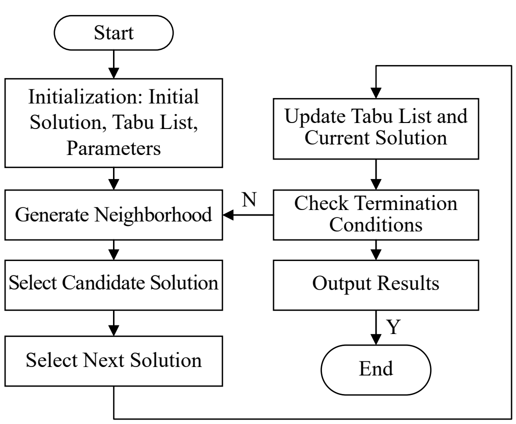

Fig. 6. Tabu search process.

Over the tabu mechanism, flexible neighbourhood definitions and release conditions, tabu search optimizes the search process and is able to find the globally optimal solution efficiently in large-scale combinatorial optimization problems.

(3) HEA-TS algorithm fusion mechanism: The integration of the HEA and TS is designed to synergistically combine their complementary strengths to enhance both the efficiency and efficacy in solving complex multi-objective optimization problems. HEA provides a robust framework for global exploration by maintaining a diverse population through its hierarchical structure and evolutionary operators (selection, crossover, and mutation), effectively preventing premature convergence. Conversely, TS contributes local exploitation capabilities by conducting intensive neighborhood searches guided by its adaptive memory (tabu list), which avoids revisiting recently explored solutions and helps escape local optima.

Within the HEA-TS framework, the HEA component is primarily responsible for broad global exploration. The main population performs wide-ranging search with high diversity, while the elite population preserves high-quality solutions for refinement. The TS module is then applied to these elite solutions, performing deep local searches to refine their quality and enhance convergence precision without becoming trapped in local optima. This hybrid mechanism ensures a balanced and efficient search strategy: HEA identifies promising regions in the solution space, and TS intensifies the search within those regions.

The tabu list in TS plays a critical role in maintaining search diversity and avoiding cyclic behavior. By recording and prohibiting recently visited solutions, it encourages exploration of uncharted areas while still allowing the search to leverage historical information. The combined approach leverages HEA's ability to explore complex, high-dimensional landscapes and TS's strength in locally intensifying search toward Pareto-optimal solutions.

The basic flow of the HEA-TS algorithm is shown in Fig. 7. The figure describes in detail the synergistic working mechanism of the hierarchical evolutionary algorithm and the tabu search, which helps to intuitively understand the combination and interaction between the two.

Through this fusion mechanism, the HEA-TS algorithm is able to give full play to the global search capability of the hierarchical evolutionary algorithm and the local optimisation advantage of the forbidden search, thus improving the solution efficiency and the search capability of the global optimal solution.

The parameter configuration of the HEA-TS algorithm in this study comprehensively references authoritative literature and extensive experience in the fields of evolutionary computation and meta-heuristic optimization, with specific settings as follows:

• Population size: Set to 100. This value is a commonly used

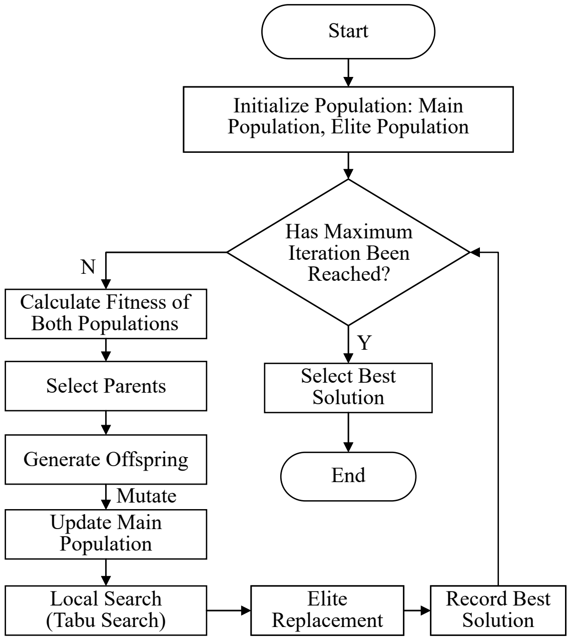

Fig. 7. HEA-TS process.

scale in genetic algorithm research, achieving a widely recognized balance between global exploration capability and computational cost [20].

• Crossover & mutation rates: The crossover probability and mutation probability are set to 0.8 and 0.1, respectively. This combination adheres to the core principle that "high-frequency crossover promotes beneficial gene recombination, while low-frequency variation maintains population diversity", and operates within the robust range validated in the literature [21].

• Tabu list size: Set to 10. This fixed-value policy follows the classical design principle of tabu search [22], striking a balance between avoiding cycles and preventing excessive restriction of the search space. It has been proven effective for medium-sized optimization problems.

All parameters are based on foundational works in the field [20], [21], [22] to ensure the benchmarking and fairness of algorithm comparisons.

(4) Adaptive local search depth mechanism: Traditional TS employs fixed iteration counts or termination criteria, failing to distinguish the potential value of different solution regions. The core of this improvement introduces a dynamic feedback adjustment mechanism based on search efficiency to the TS component, enabling adaptive adjustment of search depth according to the characteristics of the current solution region.

This mechanism dynamically adjusts the search depth for each TS iteration through two key metrics:

IR: Records the rate of solution quality improvement during consecutive TS iterations within the current elite solution neighborhood. IR is calculated as:

$$\mathrm{IR} = \frac{\mathrm{HV}_{\text{current}} - \mathrm{HV}_{\text{initial}}}{k} \tag{10}$$

where $\mathrm{HV}_{\text{initial}}$ represents the hypervolume value before the start of local search, and $\mathrm{HV}_{\text{current}}$ represents the current hypervolume value after k iterations.

SD: Search diversity evaluates the dispersion of the search space by calculating the average Euclidean distance between all candidate solutions in the current iteration:

$$\mathrm{SD} = \frac{1}{N(N-1)} \sum_{i=1}^{N-1} \sum_{j=i+1}^{N} d(X_i, X_j) \tag{11}$$

where N denotes the number of candidate solutions within the neighborhood, and $d(X_i, X_j)$ is the Euclidean distance between solution vectors X_i and X_j.

Dynamic adjustment strategy: Based on the above metrics, the dynamic adjustment strategy for the maximum iteration count $L_{\max}$ is as follows:

$$L_{\max}(t+1) = \begin{cases} L_{\max}(t)\cdot(1+\alpha), & \text{if } (\mathrm{IR} > \theta_{\mathrm{IR}}) \wedge (\mathrm{SD} > \theta_{\mathrm{SD}}) \\ L_{\max}(t)\cdot(1-\beta), & \text{if } (\mathrm{IR} < \theta_{\mathrm{IR}}) \vee (\mathrm{SD} < \theta_{\mathrm{SD}}) \\ L_{\max}(t), & \text{otherwise} \end{cases} \tag{12}$$

where θ_{IR} and θ_{SD} represent the preset thresholds for improvement rate and search diversity, respectively; α and β are depth adjustment coefficients that control the increase and decay rate of search depth, respectively; $L_{\max}(t)$ and $L_{\max}(t+1)$ denote the maximum iteration counts for the current and next iteration rounds, respectively.

This mechanism ensures the dynamic optimization of computational resources between "exploration" and "mining".

(5) Targeted elite learning strategy: Standard genetic operators (crossover and mutation) operate blindly within elite populations. The core of this enhancement lies in utilizing the distributed knowledge of the Pareto front as feedback information to guide the evolutionary direction of elite populations, thereby endowing their learning process with explicit purpose.

This strategy designs a directional cross operator based on frontier distribution density, with the following operational steps:

Density assessment: Utilize kernel density estimation methods to model the distribution density of the current non-dominated solution set within the objective space.

Crossing decision: Select two parent individuals from the elite population. If both parent individuals reside in the sparsely populated Pareto frontier region of the solution set, the DDC operator performs exploratory crossover. This involves relaxing crossover constraints to generate offspring with greater variation, thereby filling gaps in this region. If both parent individuals reside in the densely populated Pareto frontier region, the DDC operator performs refinement crossover. This involves fine-tuning within a small neighborhood to enhance solution accuracy and distribution uniformity in this area.

Adaptive adjustment: Thresholds for sparse and dense regions are dynamically updated based on each generation's non-dominated solution set, ensuring adaptive guidance.

This strategy transforms elite population evolution from random exploration to targeted efforts focused on unexplored or under-accurate regions of the true Pareto frontier.

C. Algorithm Performance Analysis

In multi-objective optimization research, the selection of benchmark problems plays a decisive role in evaluating algorithm performance. This study employs the ZDT series of test functions as a standard evaluation platform, systematically comparing four algorithms across three typical problem classes (see Table 1 for problem feature descriptions): ZDT1 (convex Pareto frontier), ZDT2 (non-convex Pareto frontier), and ZDT3 (discontinuous Pareto frontier). The algorithms compared include the GA, HEA, improved HEA-TS algorithm, and the multiobjective variant MO-CEO of the CEO algorithm.

As shown in Fig. 8, the Pareto front reveals significant differences in solution set quality among the algorithms (red: GA, green: HEA, cyan: CEO, and blue: HEA-TS). HEA-TS demonstrates optimal performance on ZDT1 and ZDT2 problems, with its solution set densely clustered near the Pareto front while maintaining good uniformity; HEA demonstrates better objective balance but lower solution accuracy than HEA-TS; GA provides a solution set with a wider distribution range but lower precision in approximating the true frontier; MO-CEO exhibits relatively dispersed solution distributions, with some solutions deviating significantly from the frontier in the ZDT3 problem.

The dynamic metric change curve diagram is shown in Fig. 9. In the Hausdorff distance convergence plot, HEA-TS consistently maintains a low value, indicating minimal extreme deviation between its solution set and the true frontier. Regarding the hypervolume metric, HEA-TS achieves the highest final convergence value, signifying its coverage of the highest-quality solution space. On the generational distance metric, HEA-TS exhibits relatively high GD values, suggesting that its convergence accuracy falls short compared to other algorithms.

Quantitative metric analysis focuses on evaluating the following three dimensions: (1) BHD reflects the maximum and minimum distances between the solution set and the true frontier, measuring extreme convergence quality; (2) HV assesses the volume of the objective space dominated by the solution set, embodying overall convergence and distribution breadth; and (3) GD represents the average distance from the solution set to the true frontier, where a smaller GD value indicates better convergence accuracy. The results in Table 2 demonstrate that HEA-TS achieves optimal performance in the hypervolume metric, showing significant improvement over the baseline GA algorithm. Its BHD metric also exhibits notable reduction across three test problems, indicating enhanced geometric consistency between the solution set and the true frontier. However, HEA-TS displays relatively high GD values, reflecting its limitations in convergence precision. This contrasts with its strong performance in other metrics and may necessitate further optimization.

Due to the introduction of the tabu search mechanism, HEA-TS requires maintaining an additional tabu list and checking the status of candidate solutions during each iteration to prevent backtracking and enhance global exploration capabilities. This results in higher computational overhead per iteration compared to traditional HEA. However, this mechanism significantly improves search efficiency, enabling the algorithm to converge to high-quality solution regions with fewer itera-

TABLE 1
OVERVIEW OF ZDT TEST PROBLEMS

Test function	Topological feature	Assessment dimensions
ZDT1	Convex Pareto Front	Basic convergence performance of optimization algorithms
ZDT2	Non-convex Pareto front	Ability to manage complex target relationships (e.g., non-linear trade-offs)
ZDT3	Multi-local optimal solution distribution	Global search capability in discontinuous Pareto spaces

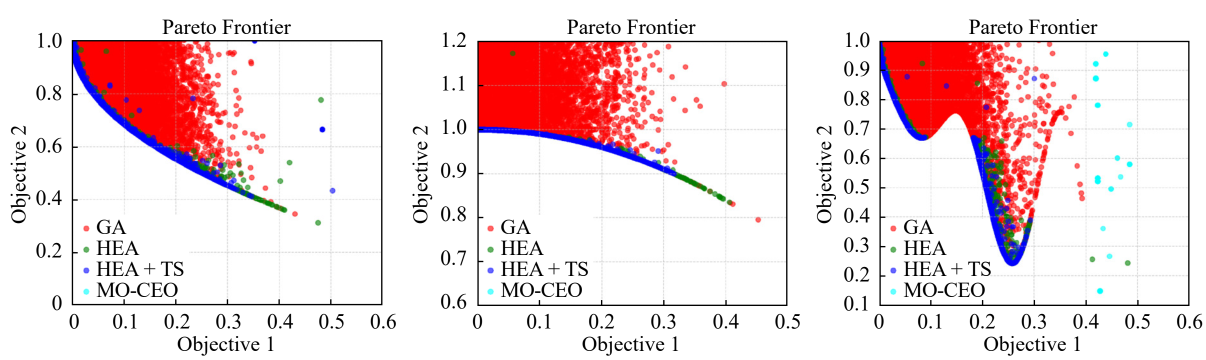

(a) ZDT1 (b) ZDT2 (c) ZDT3

Fig. 8. Analysis of test results.

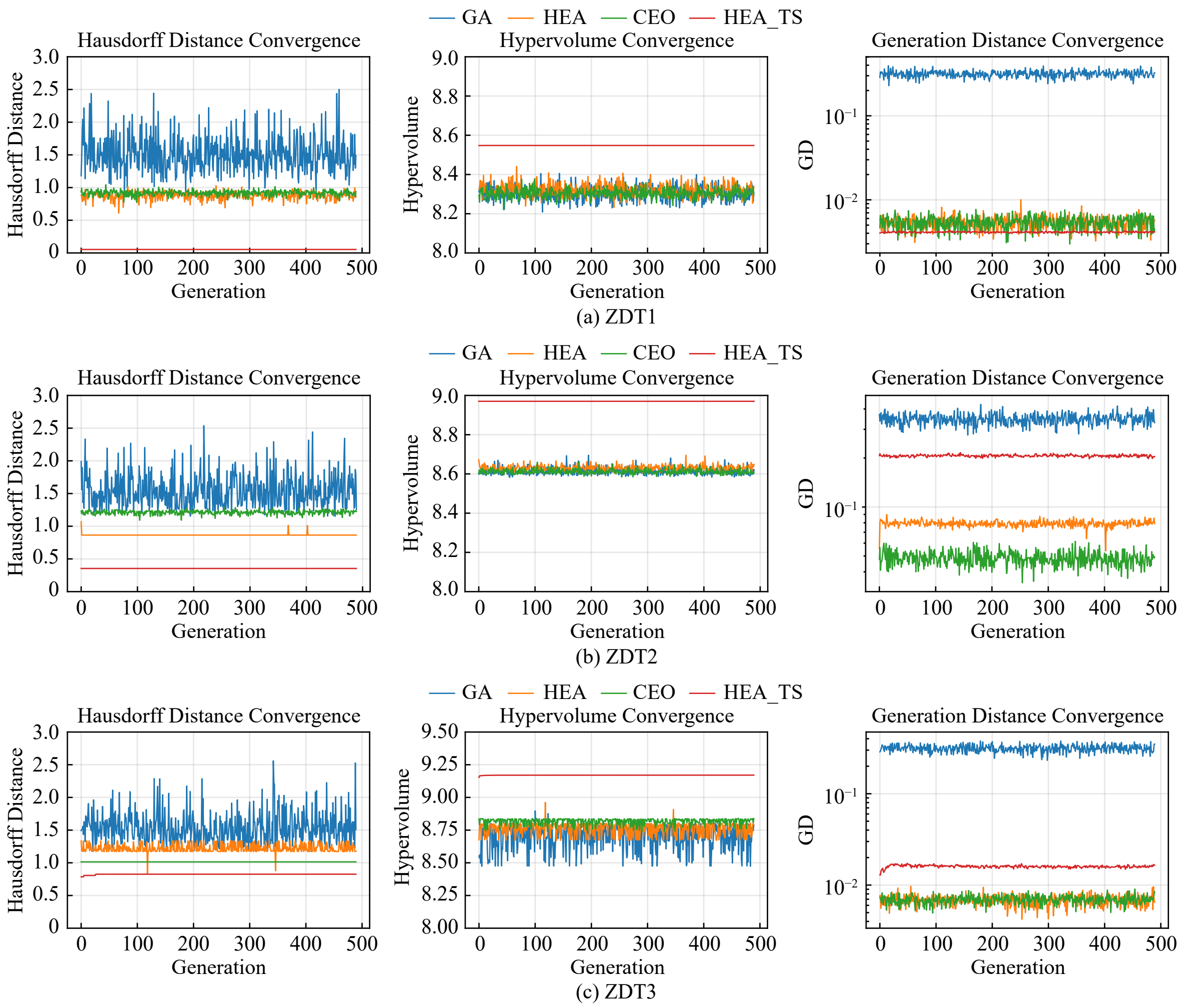

Fig. 9. Evaluation metrics comparison results.

TABLE 2
MEAN VALUES OF INDICATORS

Function	Algorithm	BHD	HV	GD
ZDT1	GA	1.51	8.28	0.328
	HEA	0.88	8.32	0.008
	CEO	0.94	8.30	0.026
	HEA_TS	0.10	8.55	0.006
ZDT2	GA	1.58	8.68	0.356
	HEA	1.19	8.69	0.053
	CEO	1.21	8.68	0.053
	HEA_TS	0.66	8.87	0.115
ZDT3	GA	1.55	4.60	0.320
	HEA	1.22	4.67	0.011
	CEO	0.84	4.77	0.010
	HEA_TS	0.82	5.04	0.022

Note: The smaller the BHD the better, the larger the HV the better, the smaller the GD the better.

tions. Consequently, it enters a stable plateau phase earlier across various metrics and achieves superior overall performance.

Comprehensive analysis indicates that the HEA-TS algorithm demonstrates favorable performance in solution set diversity and convergence stability by incorporating a tabu search mechanism, though it exhibits shortcomings in convergence accuracy (as measured by the GD metric). The MO-CEO algorithm's performance falls between traditional GAs and HEA, serving as a baseline reference, but its overall capability falls short of HEA-TS. Future research should focus on refining HEA-TS's local search strategy to reduce the GD value and enhance convergence precision.

V. MODELLING OF DISTRIBUTED ENERGY SYSTEMS

A. Distributed Power Output Modelling

The optimisation model for time-of-day tariff pricing is constructed based on the determination of time-of-day periods, taking into account the output of distributed power sources[?].

(1) Distributed wind power

Using the blades of the wind turbine to convert the kinetic energy of the wind into electrical energy, the output depends on the wind speed and is modelled as follows.

$$l_{TW,t}=\begin{cases}0 & 0\le v_t\le v_I\\ n_w\dfrac{v_t^3-v_I^3}{v_R^3-v_I^3}l_{w,S} & v_I\le v_t\le v_R\\ n_w l_{w,S} & v_R\le v_t\le v_O\\ 0 & v_O\le v_t\end{cases}\tag{13}$$

where $l_{TW,t}$ is the decentralised wind power output for the time period t; n_w is the number of decentralised wind power; v_t is the wind speed for the time period t; v_I is the cut-in wind speed; v_R is the rated wind speed; v_O is the cut-out wind speed; $l_{w,S}$ is the rated decentralised wind power output.

(2) Distributed photovoltaic

The use of photovoltaic modules to convert solar energy into electricity. The output depends on the intensity of light radiation and temperature, and the output model is as follows.

$$l_{TP,t}=n_p l_{P,S}\frac{i_t}{i_S}[1-\varepsilon_P(t_t-t_S)]\tag{14}$$

where $l_{TP,t}$ is the distributed PV output for the time period t; n_p is the number of distributed PV; $l_{P,S}$ is the rated distributed PV output under standard conditions (light radiation intensity $i_S=1000\,\mathrm{W/m^2}$, temperature $t_S=25\,°\mathrm{C}$); i_t is the light radiation intensity for the time period t; t_t is the temperature for the time period t; and ε_P is the temperature coefficient of the power (generally taken as $0.0039\,°\mathrm{C}^{-1}$).

Gas turbines. Gas turbines are commonly used in power systems to supplement renewable energy output to meet load demand. The output of gas turbines can be dynamically adjusted based on real-time load demand and wind and solar output. The output model can be expressed as:

$$P_{GT,t}=\eta_{GT}\cdot P_{GT,\text{rated}}\cdot\left(\frac{T_t}{T_{\text{rated}}}\right)^{\alpha}\cdot\left(\frac{P_{\text{fuel},t}}{P_{\text{fuel,rated}}}\right)^{\beta}\tag{15}$$

where $P_{GT,t}$ is the gas turbine output in time period t; η_{GT} is the efficiency of the gas turbine; $P_{GT,\text{rated}}$ is the rated output of the gas turbine; T_t is the temperature in time period t; T_{rated} is the standard temperature corresponding to the rated output of the gas turbine; α is the coefficient of the influence of temperature on the output; $P_{\text{fuel},t}$ is the amount of fuel supplied in time period t; $P_{\text{fuel,rated}}$ is the amount of fuel supplied corresponding to the rated output of the gas turbine; and β is the coefficient of the influence of fuel supply on the output.

(3) Distributed energy storage

Used to store excess renewable energy output and release energy when needed to balance supply and demand. The output model needs to take into account the charging and discharging efficiency, capacity limitations, and state of health of the battery. The output model can be expressed as:

$$P_{ESS,t}=\min\left(\max\left(-P_{ESS,\text{max\_dis}}\cdot P_{ESS,t},P_{ESS,\text{max\_chr}}\right)\right)\tag{16}$$

where $P_{ESS,t}$ is the output power of the energy storage system at time t (charging is negative, discharging is positive); $P_{ESS,\max\_dis}$ is the maximum discharging power of the energy storage system; and $P_{ESS,\max\_chr}$ is the maximum charging power of the energy storage system.

B. Construction of the Objective Functiong

In the time-sharing tariff optimisation problem, the reasonable construction of the objective function and the scientific definition of the constraints are the keys to ensure that the solution results have practical significance and operability.

In time-sharing tariff optimisation, it is particularly important to establish a reasonable objective function in order to balance the economic benefits and the effect of energy consumption. This objective function should not only consider the minimisation of the total cost, but also prioritise the consumption of renewable resources such as wind and solar, forming a comprehensive model for multi-objective optimisation. In this context, a multi-objective optimisation function is designed in this paper, which not only guarantees the economy of system operation, but also promotes the efficient use of clean energy. For the specific formula, see Eq. (13).

This multi-objective optimisation function prioritises the consumption of wind resources as a key objective, incorporating the need to minimise the total cost, and achieves multi-objective optimisation of the system by coordinating the balance between the utilisation of wind resources and economic costs. By assigning appropriate weights to wind-scenic consumption, the model ensures priority consumption of renewable energy in time-series tariff optimisation, thus seeking the best balance between economic and environmental benefits.

$$\begin{cases}F_r=\sum_{t=1}^{T}(P_{pv}(t)+P_{pw}(t))\\ C_{total}=C_g+C_c+C_t\\ C_g=\sum_{i\in\{pv,pw,ng,c\}}\left(c_i^v\cdot P_i^g+c_i^f\right)\\ C_c=\sum_{i\in\{pv,pw,ng,c\}}c_i^c\\ C_t=\sum_{i\in\{pv,pw,ng,c\}}E_i^e\times CP\\ F=(1-\alpha)\cdot\sum_{t=1}^{T}(P_{pv}(t)+P_{pw}(t))-\alpha\cdot C_{total}\end{cases}\tag{17}$$

where $P_{pw}(t)$ and $P_{pv}(t)$ are the total consumption of wind power and PV in time period T; C_g, C_c, and C_t are the cost of power generation, construction cost and carbon trading cost; i denotes different power generation equipment, such as photovoltaic (pv), wind power (pw), gas boiler (ng), and thermal power unit (c); c_i^v and c_i^f, c_i^c are the variable cost, fixed cost and construction cost of the i-th type of power generation equipment; P_i^g is the power generation of i-th type of equipment; E_i^e is the carbon emission of i-th type of power generation equipment; and CP is the carbon trading price.

C. Method for Determining Weighting Coefficient α

In multi-objective optimization problems, the weighting coefficient $\alpha \in [0,1]$ reflects the decision-maker's preference trade-offs among conflicting objectives (maximizing renewable energy consumption versus minimizing total cost). Its determination must adhere to scientific and objective principles, rather than subjective discretion. This paper employs a weight determination strategy based on the ideal point method [23], which integrates the decision-maker's preferences with the objective properties of the Pareto front, thereby translating subjective choices into an objective weight value.

The specific procedure for determining the weighting coefficient α is as follows (see the flowchart in Fig.:

(1) Solve single-objective ideal values: Decompose the multi-objective problem into two single-objective optimization problems and solve them separately.

• When $\alpha = 0$: Solve $\max F_r$, obtaining the ideal value for renewable energy consumption F_r^*, and record the corresponding total cost C_{total}^F.

• When $\alpha = 1$: Solve $\min C_{\text{total}}$, obtaining the ideal value for total cost C_{total}^*, and record the corresponding renewable energy consumption F_r^C.

This yields the theoretical ideal values $(F_r^*, C_{\text{total}}^*)$ and the boundary values $(F_r^C, C_{\text{total}}^F)$ for the objective functions F_r and C_{total}.

(2) Define the trade-off space: The results from Step 1 define a trade-off space:

• Renewable energy consumption can vary within the interval $[F_r^C, F_r^*]$.

• Total cost can vary within the interval $[C_{\text{total}}^F, C_{\text{total}}^*]$.

(3) Decision-maker preference selection: Based on strategic goals (e.g., prioritizing environmental protection or economic operation), the system operator specifies a desired satisfactory solution within this trade-off space, i.e., sets an expected renewable energy consumption level F_r^{set} or an acceptable total cost $C_{\text{total}}^{\text{set}}$.

(4) Calculate the weighting coefficient: Based on the decision-maker's specified expected value, the weighting coefficient α can be calculated using the following equation:

$$\alpha = \frac{F_r^* - F_r^{\text{set}}}{\left(F_r^* - F_r^{\text{set}}\right) + \left(C_{\text{total}}^{\text{set}} - C_{\text{total}}^*\right)} \tag{18}$$

This equation ensures a strict correspondence between the weight α and the decision-maker's preference. If the expected renewable energy consumption F_r^{set} is close to its ideal value F_r^* (prioritizing environmental protection), then α approaches 0. If the expected total cost $C_{\text{total}}^{\text{set}}$ is close to its ideal value C_{total}^* (prioritizing economic efficiency), then α approaches 1.

Furthermore, another commonly used method is the fuzzy decision method based on fuzzy mathematics [24]. This method involves constructing membership functions $\mu_F(F_r)$ and $\mu_C(C_{\text{total}})$ for the two objectives, normalizing them to the interval $[0,1]$, and then making decisions using the weighted sum method $(\max\{\alpha \cdot \mu_F + (1-\alpha) \cdot \mu_C\})$.

In the subsequent simulation analysis, to maintain neutrality and equally demonstrate the optimization potential of both objectives, this paper employs an equal weight strategy $(\alpha = 0.5)$ for solving and analysis. This setting serves as a baseline scenario (base case), implying that the decision-maker places equal importance on "maximizing renewable energy consumption" and "minimizing total cost".

D. Determination of Constraints

In constructing the multi-objective optimisation model, several key constraints are introduced to ensure the feasibility of the optimisation results and system stability. The first one is the power balance constraint, which is used to ensure that the system maintains a dynamic balance between power generation, energy storage, and electricity demand during all time periods to avoid the impact of load fluctuations on the grid.

$$\sum_i P_i^g + P_s = \sum_j P_j^l \tag{19}$$

where P_i^g is the amount of electricity generated by the i-th generation plant, P_s is the net power of the storage system (positive for charging and negative for discharging), and P_j^l is the load at the j-th load point, and

In order to effectively control the output characteristics of the energy storage system, the energy storage constraint mainly considers the climbing rate of the energy storage, i.e., the rate of change of charging and discharging of the energy storage should not be beyond the permissible range of the equipment in different time periods. This ramp-up constraint can avoid frequent and large power changes of the energy storage system, ensure its operation under stable working conditions, and at the same time satisfy the system's requirements for charging and discharging rates, further guaranteeing the balance and safety of the system.

$$-r_c \le \frac{P_{s,t} - P_{s,t-1}}{\Delta t} \le r_d \tag{20}$$

where r_c is the charge rate limit of the storage system; r_d is the discharge rate limit of the storage system; and Δt is the time step.

Equipment operation constraints ensure that all types of generating equipment operate within the physically and technically permissible operating limits, maintaining the overall operational stability and safety of the system.

$$P_{\min,i} \le P_i^g \le P_{\max,i} \tag{21}$$

where $P_{\min,i}$ is the minimum output power of the i-th power generation equipment; and $P_{\max,i}$ is the maximum output power of the i-th power generation equipment.

By introducing these constraints, the model can be made to optimise the objective while taking into account the actual operational requirements and constraints of the system.

E. Determination of Constraints

As shown in Fig. 10, the tariff solution is carried out by dividing the winter time period as an example, and the comparative analysis of the tariff changes between the optimised tariff scheme and the existing scheme over a 24-h period reveals the significant advantages of the optimised scheme, which implements lower tariffs during periods of lower electricity demand, effectively promotes the decentralisation of electricity consumption, and reduces the load pressure on the grid during peak hours. The optimised scheme is more cost-effective compared to the original scheme, providing economic incentives for users to adjust their electricity consumption patterns. This time-sharing tariff strategy not only improves the allocation efficiency of power resources, but also promotes changes in user behaviour through economic incentives, thus achieving optimal operation of the power system without increasing infrastructure investment. From the results, the optimised tariff scheme achieves the balance of electricity demand and the reduction of user costs through precise time slotting and tariff adjustment, demonstrating its potential value in enhancing the stability and economy of the power system. This finding provides empirical support for power market design and policy formulation, and is important for promoting the sustainable development of the power industry.

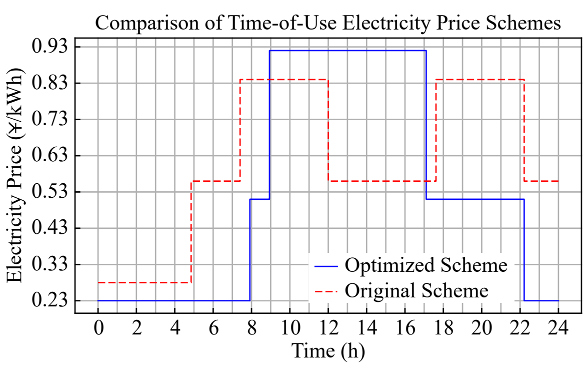

Fig. 10. Comparison of price schemes.

VI. Simulation Analysis

The simulation data for this paper were collected from the University of Terre Sainte campus, which is located in the southern coastal strip of the island of St. Pierre (geographic coordinates: 21°20′S, 55°29′E, 75 meters above sea level). The climate is typically tropical and maritime, with distinct seasonal characteristics: The rainy season (November–April) is hot and humid, and the dry season (May–October) is characterized by a high degree of humidity. It turns cool and dry under the influence of southeast trade winds (May to October). Load data: covering campus teaching area, dormitory area, and four administrative departments, with a time resolution of New energy is monitored in real time by the campus weather station, including wind speed (measured at a height of 10m from the ground), solar radiation intensity, and other parameters, synchronized with a 10-min time step.

The optimized time-sharing tariff strategy proposed in this study achieves the triple enhancement of "economy, environmental protection, and high efficiency" through the refined time slot division and the coordinated scheduling of wind and solar power. In the future, load clustering and optimization algorithms can be combined to further explore the potential of multi-energy complementarity.

In Fig. 11, comparison of load profiles shows that the original load demand curve (blue) may have higher load peaks during some hours, which usually require expensive generation or energy storage equipment to meet. The optimized TOU adjusted load demand curve (orange) shows that through reasonable tariff guidance, the load in some peak hours is reduced and the load in the trough hours is increased, which achieves peak shaving and valley filling and improves the overall efficiency of the power system. The original TOU-adjusted load demand curve (green) is in between, indicating that with the optimization of the time-sharing tariff strategy, the load adjustment effect has also been further improved.

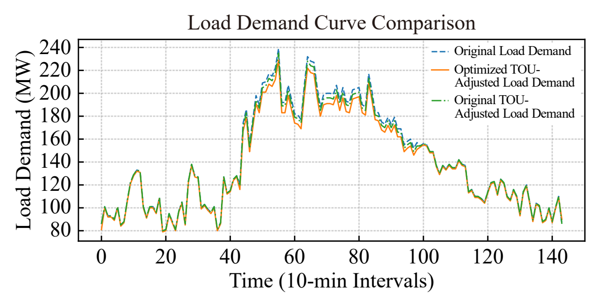

Fig. 11. Comparison of load demand curves.

The analysis of economic and environmental benefits shows (Table 3) the carbon emissions and total cost under the three strategies of original tariff, TOU tariff, and optimized TOU tariff. The data show that carbon emissions are highest under the original tariff strategy with 2474.64 kg; the TOU tariff strategy reduces carbon emissions to 2226.23 kg, a reduction of 14.08%; and the optimized TOU tariff strategy further reduces the carbon emissions to 2185.94 kg, a reduction of 11.67% compared to the original tariff and a reduction of 1.81%. In terms of total cost, the total cost under the original tariff strategy is 5876.66; the TOU tariff strategy reduces the total cost to 5830.79, a reduction of 0.78%; and the optimized TOU tariff strategy further reduces the total cost to 5784.22, which is a reduction of 1.57% compared to the original tariff, compared to the TOU tariff of 0.79%.

TABLE 3
Comparison of Carbon Emissions and Total Costs

	Original Electricity Price	TOU Price	Optimized TOU Price
Carbon Emissions (kg)	2474.64	2226.23	2185.94
Total Cost (¥)	5876.66	5830.79	5784.22

Note: The values represent the comparison of carbon emissions and total costs under different electricity pricing strategies.

Fig. 12 shows that the optimized time-of-day tariff scheme makes the power output of the equipment closer to the actual load demand (red curve). In the optimized scheme, the utilization rates of photovoltaic power generation (orange part) and wind power generation (green part) are improved, especially during the hours with abundant sunshine and wind resources, which indicates that the optimization strategy has improved the utilization efficiency of renewable energy to a certain extent. In the optimized scenario, the output power of the gas turbine (purple part) still bears a larger proportion during the peak load hours (e.g., 9 a.m. to 5 p.m.), but its output is significantly reduced during the low load hours (e.g., at night), which helps to reduce the operating cost. The energy storage device (brown part is discharging, and blue part is charging) plays a role in the optimization scheme to cut peaks and fill valleys, especially in the peak load hours, and the discharging power of the energy storage device is reasonably utilized, which reduces the dependence on the traditional power generation equipment.

As shown in Fig. 13, in pie chart (a), the cost of gas turbines accounts for 53.6% of the pie chart, indicating that traditional energy sources are more expensive to use under the original tariff scenario. The cost of photovoltaic power generation accounts for 31.8%, the cost of wind power generation accounts for 6.5%, and the cost of energy storage equipment accounts for a relatively small 8.0%. Cost composition of the optimized tariff scenario: Pie charts (b) and (c) show that in the optimized scenario, the cost of gas turbines is reduced to 48.6% to 48.1%, while the cost of PV is increased to 37.9% to 38.3%. This shows that the optimization strategy effectively promotes the use of renewable energy generation and reduces the dependence on traditional fossil energy sources, which in turn reduces the overall operating costs.

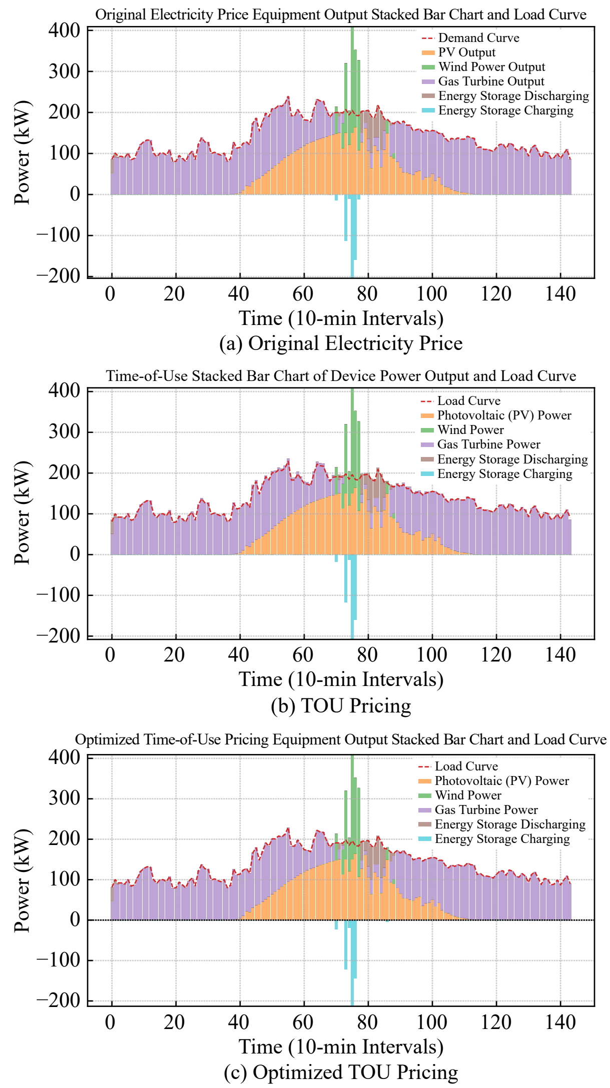

Fig. 12. Output situation and load curve of each equipment.

VII. Reach a verdict

This study addresses the challenges of time-of-use pricing optimization and load regulation in distributed energy systems by successfully establishing an innovative optimization framework that integrates supply and demand characteristics. Its effectiveness was validated through simulation. This chapter summarizes the research findings and discusses future research directions.

The main contributions of this study can be summarized in the following three aspects:

(1) Proposing an efficient HEA-TS hybrid optimization algorithm: To address the limitations of traditional multi-

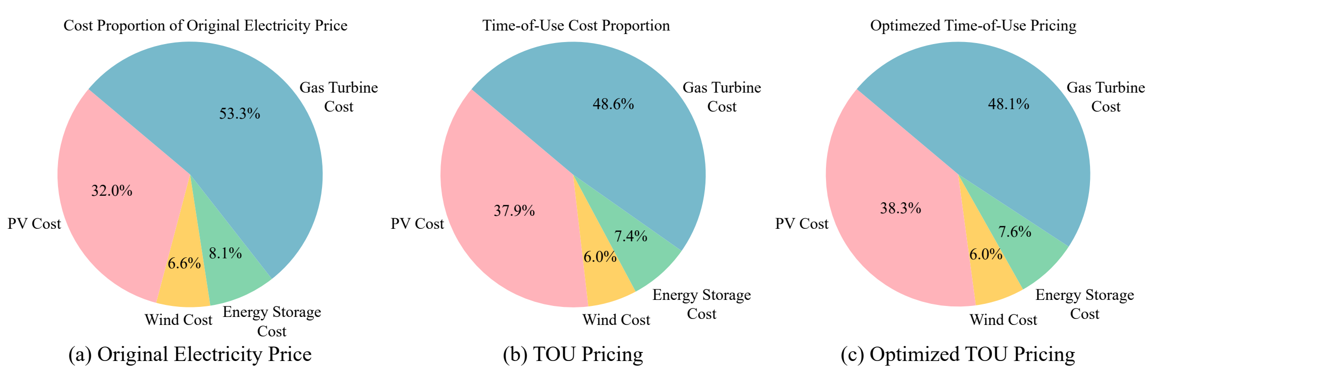

Fig. 13. Proportion of cost for each piece of equipment before and after optimisation.

objective optimization algorithms in terms of solution accuracy and efficiency, a hybrid mechanism combining HEA and TS is designed. The algorithm employs HEA for global exploration and TS for local fine-tuning, integrated with adaptive search depth and directional elite learning strategies. This significantly improves the convergence and distribution uniformity of the Pareto front, providing a new tool for optimizing complex energy systems.

(2) Establishing a supply-demand integrated TOU period classification and pricing methodology: Breaking through the traditional limitation of classifying electricity pricing periods solely based on load data, this study innovatively adopts a comprehensive feature vector for clustering analysis. This ensures that the identified peak, flat, and valley periods inherently couple the joint characteristics of high load and high renewable energy availability. Based on this, a multi-objective TOU pricing optimization model is constructed, balancing renewable energy consumption and system economy through a weight coefficient α, structurally addressing the core challenge of supply-demand mismatch.

(3) Validating the practical value of the model in promoting energy transition: Case simulation results demonstrate that the optimized TOU pricing strategy can effectively guide user electricity consumption behavior, achieving "peak shaving and valley filling" and smoothing the load curve. Ultimately, while improving grid stability, it significantly enhances renewable energy consumption rate and reduces total system operation cost and carbon emissions. This provides a replicable solution for achieving efficient and economical operation of energy systems under the "dual carbon" goals.

This study provides an effective planning-level analytical tool for the optimization of distributed energy systems. However, several limitations remain and can be further addressed in future research:

(1) Uncertainty modeling: The current model is based on deterministic scenarios. Future research will incorporate stochastic programming or robust optimization methods to comprehensively account for uncertainties in renewable generation and load demand (e.g., forecast errors), thereby enhancing the resilience and practical applicability of the scheduling strategy.

(2) Dynamic decision mechanism: In this study, the weight coefficient α is treated as a static parameter. The next step will focus on developing a dynamic and adaptive weight adjustment mechanism based on real-time system states (e.g., ultra-short-term renewable forecasts, grid carbon intensity, and market electricity prices), aiming to achieve a transition from static planning to dynamic operation.

(3) Model extension and validation: Future work will explore the applicability and effectiveness of the proposed optimization framework in broader contexts (e.g., multi-park coordination, virtual power plants, and integrated energy systems) and under different electricity market rules. Opportunities for joint testing and validation with real-world systems will also be pursued.

In summary, this study offers innovative insights and systematic solutions to address the challenges posed by the high penetration of renewable energy into the power grid. The proposed methodology and findings hold positive theoretical significance and reference value for promoting the sustainable development of the energy internet.

Declaration of Competing Interest

The authors declare that they have no known competing financial interests or personal relationships that could have appeared to influence the work reported in this paper.

Funding

This work is carried out without the support of any funding agency.

AI Usage Statement

During the preparation of this manuscript, the authors used AI-assisted tools for language polishing only. The authors have reviewed and edited the content and take full responsibility for the final version of the manuscript.

References

[1] H. G. Zhang, Y. S. Li, D. W. Gao, and J. G. Zhou, “Distributed optimal energy management for energy internet,” *IEEE Trans. Ind. Inf.*, vol. 13, no. 6, pp. 3081–3097, Dec. 2017.

[2] C. Qing and L. Yao, “Analysis and insights of significant electricity price fluctuations in Germany,” Available: URL http://www.sgeri.sgcc.com.cn/html/sgerinew/gb/xwzx/zkgd/20250424/600266202504240953000001.shtml

[3] Y. Zhang, X. C. Wei, and K. H. Feng, “Charging and Discharging Strategies of Independent Energy Storage for Distribution Grid Side Considering Distributed PV Carrying Capacity,” *China Electr. Power*, vol.57, no. 04, pp. 111-117, 2024.

[4] L. L. Wang, H. Wang, Z. Y. Ren, “Evaluation of Renewable Energy Accommodation Capacity for High Voltage Distribution Network Considering Flexible Resources Regulation Potential,” *China Electr. Power*, vol. 55, no. 10, pp.124-131, 2022.

[5] Q. Zhang, X. F. Wang, M. Fu, and J. X. Wang, “Smart grid from the perspective of demand response,” *Autom. Electr. Power Syst.*, vol. 33, no. 17, pp. 49–55, Sep. 2009.

[6] B. B. Wang, Y. Li, and C. W. Gao, “Demand side management outlook under smart grid infrastructure,” *Autom. Electr. Power Syst.*, vol. 33, no. 20, pp. 17–22, Oct. 2009.

[7] California Public Utilities Commission, “CRITICAL PEAK PRICING RATES PY 2024 STATEWIDE EVALUATION (PG&E, SCE, SDG&E) [EB/OL],” 2025. Available: https://www.cpuc.ca.gov/-/media/cpuc-website/divisions/energy-division/documents/demand-response/demand-response-workshops/2025-load-impact-protocol-workshops/statewide-cpp-presentation.pdf

[8] O. Corradi, H. Ochsenfeld, H. Madsen, and P. Pinson, “Controlling electricity consumption by forecasting its response to varying prices,” *IEEE Trans. Power Syst.*, vol. 28, no. 1, pp. 421–429, Feb. 2013.

[9] Z. S. Zhang and D. L. Yu, “RBF-NN based short-term load forecasting model considering comprehensive factors affecting demand response,” *Proc. CSEE*, vol. 38, no. 6, pp. 1631–1638, Mar. 2018.

[10] H. Z. Li, R. Z. Cao, and X. Y. Zhang, “Demand response model based on real time pricing in household electricity consumption,” *J. Power Syst. Autom.*, vol. 30, no. 11, pp. 26−31+51, 2018.

[11] P. D. Huang, H. X. Zhan, G. B. Peng, and Y. H. Chen, "The model of wind power accommodation considering source network load on each side benefits in TOU price," *Electr. Meas. Instrum.*, vol. 54, no. 7, pp. 53–58, Apr. 2017.

[12] K. Deb and H. Jain, "An evolutionary many-objective optimization algorithm using reference-point-based nondominated sorting approach, Part I: solving problems with box constraints," *IEEE Trans. Evol. Comput.*, vol. 18, no. 4, pp. 577–601, Aug. 2014.

[13] L. T. Qiao, T. Wang, and J. N. Liu, "Distribution network reactive power optimization considering generation network load storage interaction," *Electrical Measurement & Instrumentation*, 2024, vol. 61, no. 05, pp.146-151+189.

[14] B. Zhou, R. Yang, C. B. Li, Y. J. Cao, Q. Wang, and J. Liu, "Multiobjective model of time-of-use and stepwise power tariff for residential consumers in regulated power markets," *IEEE Syst. J.*, vol. 12, no. 3, pp. 2676–2687, Sep. 2018.

[15] M. H. Albadi and E. F. El-Saadany, "A summary of demand response in electricity markets," *Electr. Power Syst. Res.*, vol. 78, no. 11, pp. 1989–1996, Nov. 2008.

[16] H. R. Varian, *Intermediate Microeconomics: A Modern Approach*, New York: Norton, 2003.

[17] P. Wang, Y. W. Ma, Z. Q. Ling, and G. H. Luo, "Peak-valley period partition and abnormal time correction for time-of-use tariffs under daily load curves based on improved fuzzy c-means," *IET Gener. , Transm. Distrib.*, vol. 17, no. 24, pp. 5396–5409, Dec. 2023.

[18] X. L. Ju and F. Liu, "Wind farm layout optimization using self-informed genetic algorithm with information guided exploitation," *Appl. Energy*, vol. 248, pp. 429–445, Aug. 2019.

[19] R. Chandran, S. R. Kumar, and N. Gayathri, "Genetic algorithm-based tabu search for optimal energy-aware allocation of data center resources," *Soft Comput.*, vol. 24, no. 21, pp. 16705–16718, Aug. 2020.

[20] K. Deb, "Multi-objective optimisation using evolutionary algorithms: an introduction," in *Multi-Objective Evolutionary Optimisation for Product Design and Manufacturing*, L. H. Wang, A. H. C. Ng, and K. Deb, Eds. London: Springer, 2011, pp. 3–34.

[21] K. Deb, A. Pratap, S. Agarwal, and T. Meyarivan, "A fast and elitist multiobjective genetic algorithm: NSGA-II," *IEEE Trans. Evol. Comput.*, vol. 6, no. 2, pp. 182–197, Apr. 2002.

[22] M. Gendreau and J. Y. Potvin, "Tabu search," in *Search Methodologies: Introductory Tutorials in Optimization and Decision Support Techniques*, E. K. Burke and G. Kendall, Eds. Boston: Springer, 2014, pp. 243–263.

[23] K. Deb and J. Sundar, "Reference point based multi-objective optimization using evolutionary algorithms," in *Proceedings of the 8th Annual Conference on Genetic and Evolutionary Computation*, 2006, pp. 635–642.

[24] H. J. Zimmermann, "Fuzzy programming and linear programming with several objective functions," *Fuzzy Sets Syst.*, vol. 1, no. 1, pp. 45–55, Jan. 1978.

Xiuyu Zhang was born in Jilin City, China. He received the B.S. and M.S. degrees from Northeast Electric Power University, Jilin, China, in 2003 and 2006, respectively, and the Ph.D. degree from Beijing University of Aeronautics and Astronautics (BUAA), Beijing, China, in 2012. He is currently a Professor with the School of Automation Engineering, Northeast Electric Power University, Jilin, China. His research interests include robust and adaptive control for nonlinear systems.

Jin Sun was born in Henan Province, China. He received his B.S. degree from Luoyang Institute of Science and Technology, Luoyang, China, in 2019. He is currently a master's student in Control Engineering at the School of Automation Engineering, Northeast Electric Power University, Jilin, China. His research interests include optimization and scheduling of microgrids.

Xinkai Chen received his Ph.D. degree in engineering from Nagoya University, Japan, in 1999. He is currently a professor in the Department of Electronic and Information Systems, Shibaura Institute of Technology, Japan. His research interests include adaptive control, smart materials, hysteresis, sliding mode control, machine vision, and observer. He has served as an Associate Editor of several journals, including IEEE Transactions on Automatic Control, IEEE Transactions on Control Systems Technology, IEEE/ASME Transactions on Mechatronics, European Journal of Control, etc. He has also severed for international conferences as organizing committee members including Program Chairs, Program Co-Chairs, etc.

Lincheng Han received his B.S. degree in computer science and technology from Hebei Normal University, China, in 2008, his M.S. degree in computer application technology from the Academy of Armored Forces Engineering of PLA, Beijing, China, in 2010, and his Ph.D. degree in control science and engineering from Northeast Electric Power University, Jilin, China, in 2025. He was a Lecturer at the PLA Army Infantry Academy, Shijiazhuang Campus, China, from 2015 to 2020. His research interests include machine learning, deep learning, Bayesian theory, and smart grid applications.